Influence of alloying additions on grain boundary cohesion of transition metals: First-principles determination and its phenomenological extension

W. T. Geng and A. J. Freeman
Department of Physics and Astronomy, Northwestern University, Evanston, Illinois 60208

G. B. Olson
Department of Materials Science and Engineering, Northwestern University, Evanston, Illinois 60208
(Received 12 June 2000; published 3 April 2001)

The toughness and ductility of ultrahigh-strength alloys is often limited by intergranular embrittlement, particularly under conditions of unfavorable environmental interactions such as hydrogen embrittlement and stress corrosion cracking. Here we investigated the mechanism by which the segregated substitutional additions cause intergranular embrittlement. An electronic level phenomenological theory is proposed to predict unambiguously the effect of a substitutional alloying addition on grain boundary cohesion of metallic alloys, based on first-principles full-potential linearized augmented plane-wave method (FLAPW) calculations on the strengthening and embrittling effects of the metals Mo and Pd on the Fe grain boundary cohesion. With the bulk properties of substitutional alloying addition A and the matrix element M as inputs, the strengthening or embrittling effect of A at the grain boundary of M can be predicted without carrying out first-principles calculations once the atomic structure of the corresponding clean grain boundary is determined. Predictions of the embrittlement potency of a large number of metals, including the $3d$, $4d$, and $5d$ transition metals, are presented for the Fe $\Sigma 3$ (111) and the Ni $\Sigma 5$ (210) grain boundaries. Rigorous FLAPW calculations on the effect of Co, Ru, W, and Re on the Fe $\Sigma 3$ (111) grain boundary and Ca on the Ni $\Sigma 5$ (210) grain boundary cohesion confirm the predictions of our model. This model is expected to be applicable to other high-angle boundaries in general and instructive in the quantum design of ultrahigh-strength alloys with resistance to intergranular fracture.

DOI: 10.1103/PhysRevB.63.165415 PACS number(s): 68.35.Gy, 68.35.Ct, 73.20.At, 73.20.Hb

I. INTRODUCTION

Grain boundary cohesion is often the controlling factor limiting the ductility of high-strength metallic alloys.[1] Thus, understanding the influence of transition metal alloying additions is of great importance in predicting and controlling grain boundary embrittlement (GBE) since the complexity of GBE behavior is often associated with the presence of substitutional alloying elements. Attempts at qualitatively explaining GBE on the electron-atom level go back to the 1960's.[2] Although predictions based on simple thermodynamic[3–5] and pair bonding models[6,7] have been proposed, the role of alloying elements on the cohesion of grain boundaries in alloys remains controversial. A thermodynamic theory by Rice and Wang[8] demonstrated that previous thermodynamic models are incorrect and identified the key surface-thermodynamic energy difference governing the quantitative role of a boundary segregant. In addition to the simple pair-bonding approaches,[6,7] which, like thermodynamic theories, employ energetics to describe the effect of segregants, electronic structure theorists have applied both empirical[9,10] and first-principles quantum-mechanical methods[11,12] in attempts to directly deduce the effect of segregants on grain boundary (GB) fracture resistance. In contrast to these studies, our recent line of research[13–17] has applied rigorous first-principles methods to evaluate the surface-thermodynamic energy difference identified by Rice and Wang as directly connected to the ideal work of GB fracture.

In spite of the complexity of the mechanical behavior and GB atomic structures, general trends in certain mechanical properties can be correlated with specific features of the electronic structure.[12,18] First-principles computation has proved to be an accurate and powerful tool in attacking the problem of the mechanical properties of real materials such as GBE. An inherent advantage of the first-principles electronic theory is that it is independent of any adjustable parameters, and so, numerical results provide a solid basis or starting point for phenomenological theories. Without such a theory starting from first-principles, one has always to repeat the full procedure of calculations to predict quantitatively the effect of any substitutional element even on the same GB.[15,17] In this sense, the exact mechanism by which segregation elements cause embrittlement remains unclear.

Very recently,[17] the effect of Mo and Pd substitutional segregation on the cohesion of the Fe $\Sigma 3$ (111) GB was investigated using the first-principles full-potential linearized augmented plane wave[19] (FLAPW) total energy/atomic force method with the generalized gradient approximation (GGA).[20] Based on the Rice-Wang model,[8] our total energy calculations show that Mo has a significant beneficial effect on the Fe GB cohesion, while Pd behaves as a weak embrittler. An analysis of the geometry optimization indicates that both Mo and Pd have a moderate atomic size to fit well in the GB substitutional site. The elastic energy associated with the Mo and Pd segregation was estimated with a rigid environment approximation. It was found that both Mo and Pd introduce a beneficial volume effect. Studies of the electronic structures show that the strong bonding capability associated

with its half-filled *d* bands makes Mo a cohesion enhancer (-0.90 eV) for the Fe $\Sigma 3$ (111) GB. By comparison, the weak bonding capability associated with its filled *d* bands leads Pd to be a weak embrittler ($+0.08$ eV). These first-principles quantum-mechanical results support, in general, the main idea of the simple pair-bonding models[6,7] in that the elemental cohesive energy difference between the alloying element and the host element plays an important role in determining the effect of this alloying element on the host GB cohesion. They differ, however, quite significantly: For example, for Mo and Pd in the Fe GB, the embrittlement potency given by Seah's pair-bonding model[6] is -1.5 and $+0.9$ eV, respectively. This significant difference with the values of -0.90 and $+0.08$ eV from our rigorous calculations indicates that a quantum-mechanical treatment is necessary in an accurate study of the GBE. Also, the numerical results for Pd, which has a similar elemental cohesive energy to that of Fe, point to the importance of the role played by the GB free volume, which can be determined with high accuracy only by quantum-mechanical calculation.

Based on the physical insight obtained from the results of our rigorous calculations, here we develop a phenomenological model by which the embrittlement potency of a substitutional atom in a given GB can be predicted without carrying out full first-principles calculations. To be accurate and reliable, such a theory must use first-principles results, rather than adjustable parameters, as inputs. To be capable of prediction without solving the quantum-mechanical Schrödinger equation, such a theory must also make use of atomic, or bulk quantities as inputs. This means that this model should have an electronic, rather than an atomistic or thermodynamic basis, in order to yield a quantum description of the mechanical behavior of a substitutional element at the GB. The rest of the paper is organized as follows. In Sec. II, the development of a phenomenological model starting from first-principles is presented. Confirmation of the model with rigorous FLAPW calculations is discussed in Sec. III, and in Sec. IV, we give a short summary.

II. PHENOMENOLOGICAL MODEL

A. Volume effect

Since a segregant can introduce a significant relocation of the atoms near the GB,[16] the volume effect of a segregant is of great importance for understanding many of its physical and mechanical properties at the GB. In a highly precise first-principles treatment, one has to fully relax the atoms near the GB.

To address the problem of volume mismatch, the atomic size of the segregant and also the size of the GB site should be well defined. Unfortunately, the geometric size of an atom has no absolute meaning and its definition depends on the physical, chemical, or mechanical problem under consideration. The problem of defining the size of an atom in metallic solid solutions was discussed in detail by King[22] in the study of substitutional solid solutions. One of these definitions uses the atomic volume in the structure of the elemental crystals and was adopted by de Boer *et al.*[23] in the study of energy effects in transition metal alloys and solid solutions. In our view, the substitutional alloying additions segregated to the GB core can be taken as a special kind of solid solution. Thus, in the current paper, we also employ this definition.

Volume expansion (or ''free volume'') is an important property in the atomic structure of the GB. Its contribution to the space available for the substitutional element has a significant influence on the physical and mechanical behavior of this element.[17] The existence of GB volume expansion makes the problem of the volume effect in the GB different from those in the alloys and solid solutions, where the otherwise undisturbed atomic structure is perfect. The FLAPW method employed in our investigations (e.g., Refs. 13 and 15–17 is well known for both its high precision and computational effort. To simulate an Fe $\Sigma 3$ (111) or Ni $\Sigma 5$ (210) GB, more than 20 atoms need to be included in a calculational unit cell. And the transition metals, especially those with magnetism such as Fe and Ni, are known to have a poor convergence in solving the Kohn-Sham equation self-consistently. Therefore, we relaxed the atomic positions only in the direction normal to the GB plane and kept the lateral symmetry and also the mirror symmetry in the normal direction, which is thought to be a reasonable approximation as we achieved fairly good agreement with the experiment on the mechanical behavior of the impurities[13,16] and additions.[15,17] Therefore, our measure for the GB expansion involves only the relative normal displacements. A local measure for the GB expansion is the relative normal displacement of the two nearest atoms, $M(2)$ across the boundary plane as represented in Figs. 1(a) and 2(a). This definition, however, is not appropriate for the investigation of the volume mismatch between the substitutional element and the GB site, as the relocation of the atoms near the GB involves $M(4)$, which, along with $M(2)$ and $M(3)$, determines the local environment of the GB core. The volume of the GB site, V^{GB}, can be taken as the displacements of $M(4)$. The calculated V^{GB} for the Fe $\Sigma 3$ (111) GB is 27.4 a.u.^{3} (34.5% of the bulk value,[24] 79.4 a.u.^{3}); for the Ni $\Sigma 5$ (210), it is 18.6 a.u.^{3} (25.2% of the bulk value,[24] 73.8 a.u.^{3}).

In a very recent work, Ochs *et al.*[25,26] studied the atomic structures for the $\Sigma 5(310)$ GB in bcc Nb, Mo, Ta, and W with the first-principles pseudopotential method. For Nb, Mo, and W, their calculations indicate noticeable lateral displacements of the grains. Based on their first-principles results, we might suppose that lateral atomic displacements in cases of $3d$ transition metals such as Fe and Ni can also possibly lower the total energy of the GB. If this is the case, a more precise measure of the GB expansion in Fe and Ni should also consider the lateral displacements of the GB atoms as well.

As we have pointed out previously,[17] not all the expanded volume near the GB is *available* for the GB core atom. The GB core atom $A/M(1)$ can form bonds only with $M(2)$ and $M(4)$, but not with $M(3)$. This means that only two-thirds of the GB free volume per site is available for $A/M(1)$. Thus, the volume mismatch ΔV^A between a segregant and the GB can be defined as

$$\Delta V^A \equiv V^A - \left(V^M + \tfrac{2}{3} V^{GB} \right). \tag{1}$$

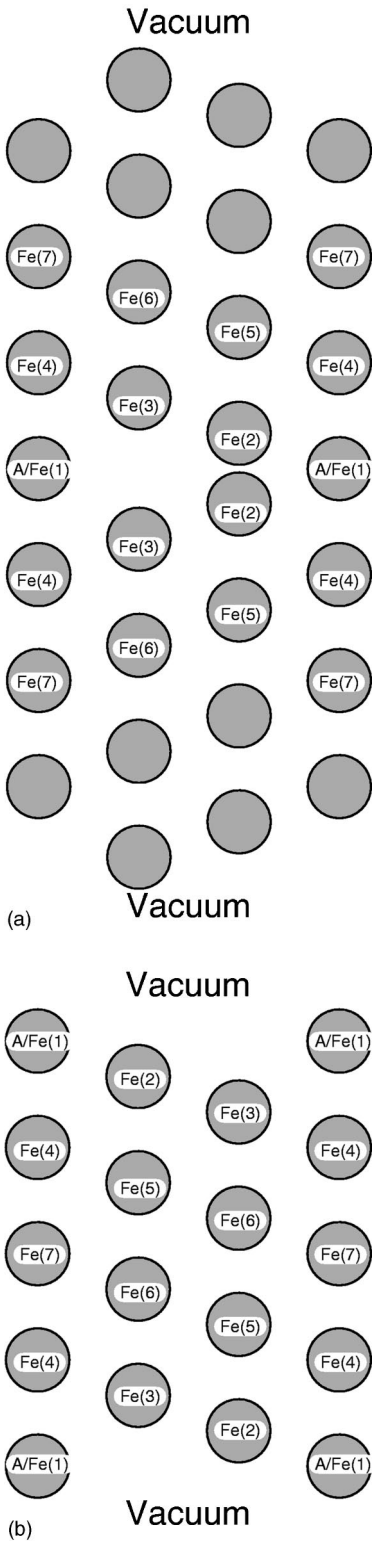

FIG. 1. Model and notation for the structure of (a) the Fe $\Sigma 3$ (111) [001] grain boundary, and (b) the Fe (111) free surface.

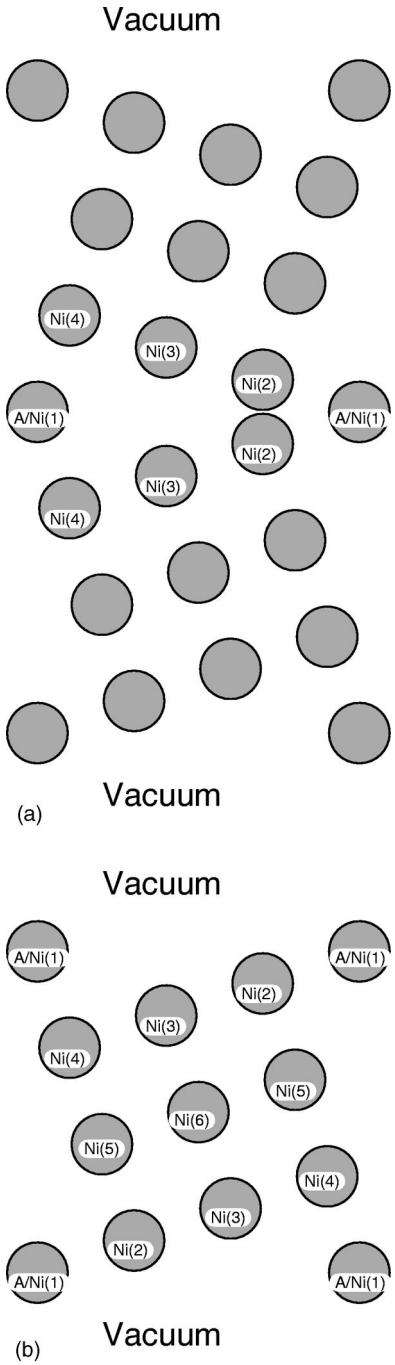

FIG. 2. Model and notation for the structure of (a) the Ni $\Sigma 5$ (210) [001] grain boundary, and (b) the Ni(210) free surface.

To address the volume effect of a substitutional addition *A*, one should compare the elastic energy of the clean and segregated GB. This elastic energy is associated with the volume mismatch between $A/M(1)$ and the GB site. Since the crystal lattice near the GB is not perfect even without the volume mismatch between $A/M(1)$ and the GB site, the bulk modulus and shear modulus (of M) near the GB no longer retain the perfect bulk values and are not well-defined. As an approximation, these deviations are neglected in the present model. In our previous work,[17] we employed a rough approximation to estimate the elastic energy associated with the volume mismatch between $A/M(1)$ and the GB site. We neglected the relaxation of the GB during segregation and took the effect of the volume mismatch between the GB core atom and the GB hole as only the compression or expansion of the segregant in a rigid environment. As an improvement,

we now calculate the elastic energy in the framework of a classical elasticity theory with the *sphere and hole* model developed by Friedel and Eshelby.[27] In this model, a spherical hole with volume V^M (atomic cell of metal M) in the matrix is partly filled by a sphere of metal A with volume V^A (dissolved atomic cell). The remaining volume, $(V^M - V^A)$, is accommodated by elastic deformation of M and A. If this is a state of purely internal stress, the total volume is unaffected. Both A and hole are then subjected to a uniform hydrostatic pressure. The stress on A is related to its bulk modulus K_A, while that on the matrix is related to an effective modulus equal to 4/3 times the shear modulus of the matrix,[27] G_M.

The elastic energy yields

$$E_V^A = \frac{K_A(\Delta V^A)^2}{2V^A} + \frac{2G_M(\Delta V^M)^2}{3V^M}, \tag{2}$$

where ΔV^A and ΔV^M are the volume changes of sphere and hole due to the internal stress. The pressures are adjusted such that they are continuous across the interface between matrix and ''inclusion,'' which leads to an expression for the elastic energy per mole of the solute metal

$$E_V^A = \frac{2K_A G_M (V^M - V^A)^2}{3K_A V^M + 4G_M V^A}. \tag{3}$$

In the GB environment, the hole cut from the matrix has a volume $V^M + 2/3V^{GB}$ rather than V^M. Therefore, to describe the GB case, Eq. (3) should take the form,

$$E_V^A = \frac{2K_A G_M \left(V^A - V^M - \frac{2}{3} V^{GB} \right)^2}{3K_A V^M + 4G_M V^A}. \tag{4}$$

$A = M$ corresponds to the clean GB case,

$$E_V^M = \frac{8K_A G_M (V^{GB})^2}{27K_A V^M + 36G_M V^A}. \tag{5}$$

When $M(1)$ is replaced by A, the change of the elastic energy near the GB core, ΔE_V^A, is

$$\Delta E_V^A = E_V^A - E_V^M, \tag{6}$$

which is the volume elastic effect of a substitutional addition A in the GB core site.

We calculated ΔE_V^A for a large number of metals, including the $3d$, $4d$, and $5d$ transition metals on the Fe $\Sigma 3$ (111) and the Ni $\Sigma 5$ (210) GB. The calculated ΔE_V^A value for each alloying addition is listed in column 8, Tables I and II. A positive value represents an increase of the elastic energy near the GB, and so, this segregant is not favored energetically. It is seen that for both the Fe $\Sigma 3$ (111) and the Ni $\Sigma 5$ (210) GB, simple metals (except for Li and Al) introduce harmful volume effects, due to their large atomic size. Most transition metals have a moderately larger atomic size compared to Fe and Ni and introduce a beneficial volume effect to the GB cohesion. For instance, the volume effects of Mo and Pd in the Fe $\Sigma 3$ (111) GB are -0.09 and -0.11 eV, respectively. If the GB hole gets to be, say 10% smaller due to the lateral relaxation, these volume effects would be -0.06 and -0.09 eV, about 20–30 % smaller. In Seah's pair-bonding model,[6] volume expansion of the GB is not considered.

B. Bonding character

The other factor, even more important in general, in determining the behavior of a segregant in the GB is its bonding character in both the GB and free surface (FS) environments. At the electronic level, a quantitative description of the chemical bonding will generally employ the concepts of charge transfer, or electronegativity. However, neither charge transfer nor electronegativity is well-defined in a nonelemental crystal and therefore is not useful to build into a unified theory. The macroscopic quantity that can be a measure of the bonding capability of an element, as adopted in the simple thermodynamic[5] or pair-bonding theory[6] of GBE, is the elemental cohesive energy. It is also employed in the present model.

According to the Rice-Wang thermodynamic theory, the potency of a segregation impurity in reducing the ''Griffith work'' of a brittle boundary separation is a linear function of the difference in *binding energies* for that impurity at the GB and the FS. For a substitutional addition, the above *binding energies* should be binding energy differences between the segregant and the host (GB core) atom. As discovered in our previous work (cf. Table III in Ref. 17, the first-principles FS and GB (Fe $\Sigma 3$) chemical energies, defined as the work needed to remove the segregant while not permitting the host (Fe) atoms to relax, have a simple relation

$$E_{Chem}^{FS}(A) \simeq \frac{2}{3} E_{Chem}^{GB}(A). \tag{7}$$

Thus, the difference in *binding energies* for A at the GB and the FS, E_{Chem}^A, is then

$$E_{Chem}^A \simeq \frac{1}{3} E_{Chem}^{GB}(A). \tag{8}$$

From Table III in Ref. 17, it is also found[17] that

$$E_{Chem}^{GB}(A) - E_{Chem}^{GB}(M) \simeq E_{Coh}^A - E_{Coh}^M. \tag{9}$$

Combining Eqs. (7) and (9), we have

$$\Delta E_{Chem}^A \equiv E_{Chem}^A - E_{Chem}^M \simeq \frac{1}{3}(E_{Coh}^A - E_{Coh}^M). \tag{10}$$

This means that the embrittlement potency of a substitutional atom in the GB of Fe is about 1/3 of the cohesive energy difference between that element and the host Fe atom if the volume effect is not significant. We note that in Seah's pair-bonding model, this factor is 1/2. This difference indicates that a quantum mechanical treatment is necessary in an accurate study of the GBE. The factor 1/3 can be understood by the $\sqrt{Z}$ theory.[28,29] The simplest expression of band character is in the second-moment approximation to the tight-binding model, in which the cohesive energy per atom varies

TABLE I. Model calculated [cf. Eq. 15] embrittling effect ΔE_B^A (eV) for all of the transition elements on the Fe $\Sigma 3$ grain boundary cohesion. Also listed are elemental cohesive energies E_{Coh}^A and ΔE_{Coh}^A (eV), heat of formation of solid solution AFe ΔE_{Heat}^A, atomic volumes V^A, and volume mismatch ΔV^A (a.u.^{3}), bulk moduli K (10^{11} N/m^2), volume mismatch correction $\delta\Delta E_V$, and also the work needed to change the ground fcc (hcp is approximated by fcc) structure to bcc structure for an element. The shear modulus of Fe, G_{Fe}, is (Ref. 31) 0.816×10^{11} N/m^2.

Atom	$-E_{Coh}^A$	ΔE_{Coh}^A	ΔE_{Heat}^A	ΔE_{Stru}	V^A	K_A	$\delta\Delta E_V^A$	ΔE_B^A
Li	1.63	2.66	0.94	0.00	143.58	0.116	−0.04	1.16
Be	3.32	0.97	−0.20	0.03	55.77	1.003	0.44	0.71
Na	1.11	3.18	2.75	0.00	254.46	0.068	0.18	2.16
Mg	1.51	2.78	0.67	0.01	156.93	0.354	0.19	1.34
Al	3.39	0.90	−0.91	0.12	112.09	0.722	−0.07	−0.03
K	0.93	3.36	4.80	0.00	481.33	0.032	0.33	3.05
Ca	1.84	2.45	1.28	0.01	293.40	0.152	0.76	2.01
Sc	3.93	0.36	−0.52	0.04	158.04	0.435	0.26	0.22
Ti	4.86	−0.57	−0.74	0.02	119.22	1.051	−0.01	−0.44
V	5.30	−1.01	−0.29	0.00	93.46	1.619	−0.11	−0.54
Cr	4.10	0.19	−0.06	0.00	81.01	1.901	−0.02	0.02
Mn	2.98	1.31	0.01	*	82.49	0.596	−0.07	0.37
Fe	4.29	0.00	0.00	0.00	79.39	1.683	0.00	0.00
Co	4.39	−0.10	−0.02	0.20	75.23	1.914	0.07	0.10
Ni	4.44	−0.15	−0.06	0.06	73.83	1.86	0.09	0.04
Cu	3.50	0.79	0.50	0.01	79.86	1.37	−0.01	0.42
Zn	1.35	2.94	−0.14	0.07	103.02	0.598	−0.11	0.85
Rb	0.85	3.44	4.75	0.00	587.83	0.031	0.47	3.20
Sr	1.72	2.57	1.90	0.00	379.12	0.116	0.97	2.46
Y	4.39	−0.10	−0.06	0.09	223.45	0.366	0.92	0.90
Zr	6.32	−2.03	−1.17	0.01	157.30	0.833	0.47	−0.59
Nb	7.47	−3.18	−0.70	0.00	121.37	1.702	0.05	−1.24
Mo	6.81	−2.52	−0.09	0.00	105.11	2.725	−0.09	−0.96
Tc	6.85	−2.56	−0.13	0.19	95.85	2.97	−0.11	−0.94
Ru	6.62	−2.33	−0.20	0.53	91.68	3.208	−0.10	−0.77
Rh	5.75	−1.46	−0.23	0.36	92.95	2.704	−0.10	−0.54
Pd	3.94	0.35	−0.19	0.08	99.24	1.808	−0.11	−0.03
Ag	2.96	1.33	1.23	0.00	115.35	1.007	−0.04	0.81
Cd	1.16	3.13	0.42	0.04	145.43	0.467	0.15	1.35
Cs	0.83	3.46	5.21	0.00	745.67	0.020	0.40	3.29
Ba	1.86	2.43	2.12	0.00	421.77	0.103	1.04	2.56
La	4.49	−0.20	0.25	0.11	249.93	0.243	0.84	0.89
Hf	6.35	−2.06	−0.98	0.10	149.29	1.09	0.43	−0.55
Ta	8.09	−3.80	−0.67	0.00	148.31	2.00	0.61	−0.88
W	8.66	−4.37	0.00	0.00	107.11	3.232	−0.08	−1.54
Re	8.10	−3.81	−0.01	0.27	99.24	3.72	−0.11	−1.29
Os	8.10	−3.81	−0.17	0.85	94.51	4.18	−0.11	−1.15
Ir	6.93	−2.64	−0.38	0.64	95.58	3.55	−0.11	−0.91
Pt	5.85	−1.56	−0.59	0.16	101.93	2.783	−0.11	−0.77
Au	3.78	0.51	0.37	0.00	114.37	1.732	−0.03	0.26
Hg	0.69	3.60	0.69	*	158.41	0.382	0.22	1.65
Tl	1.87	2.42	1.06	0.00	192.80	0.359	0.55	1.71
Pb	2.04	2.25	0.95	0.00	204.49	0.430	0.81	1.88

as $\sqrt{Z}$, where Z is the atomic coordination that can range from 1 (diatomic molecule) to 12 (fcc crystal). For the segregant in the Fe $\Sigma 3$ (111) GB, $Z=8$, and for that on the Fe (111) FS, $Z=4$. Hence, by applying the $\sqrt{Z}$ rule, one will get

$$E_{Chem}^A \simeq 0.293\times E_{Chem}^{GB}(A). \tag{11}$$

The relation is treated as approximate rather than exact because in both FS and GB systems, the bond lengths of

TABLE II. Model calculated [cf. Eq. 15] embrittling effect ΔE_B^A (eV) for all of the transition elements on the Ni $\Sigma 5$ grain boundary cohesion. Also listed are elemental cohesive energies E_{Coh}^A and ΔE_{Coh}^A (eV), heat of formation, heat of solid solution ANi ΔE_{Heat}^A, atomic volumes V^A, and volume mismatch ΔV^A (a.u.^{3}), bulk moduli K (10^{11} N/m^2), volume mismatch correction $\delta\Delta E_V$, and also the work needed to change the ground bcc structure to fcc (hcp is approximated by fcc) structure for an element. The shear modulus of Ni, G_{Ni}, is (Ref. 31) 0.839×10^{11} N/m^2.

Atom	$-E_{Coh}^A$	ΔE_{Coh}^A	ΔE_{Heat}^A	ΔE_{Stru}	V^A	K_A	$\delta\Delta E_V^A$	ΔE_B^A
Li	1.63	2.81	0.03	0.02	143.58	0.006	−0.04	0.99
Be	3.32	1.12	−0.22	0.00	55.77	1.003	0.27	0.57
Na	1.11	3.33	1.40	0.01	254.46	0.068	0.27	1.85
Mg	1.51	2.93	−0.25	0.00	156.93	0.354	0.36	1.25
Al	3.39	1.05	−1.39	0.00	112.09	0.722	0.06	−0.05
K	0.93	3.51	2.35	0.00	481.33	0.032	0.40	2.35
Ca	1.84	2.60	−0.37	0.00	293.40	0.152	0.91	1.65
Sc	3.93	0.51	−1.79	0.00	158.04	0.435	0.46	0.03
Ti	4.86	−0.42	−1.54	0.00	119.22	1.051	0.18	−0.47
V	5.30	−0.86	−0.75	0.17	93.46	1.619	−0.05	−0.53
Cr	4.10	0.34	−0.27	0.39	81.01	1.901	−0.05	0.10
Mn	2.98	1.46	−0.33	0.00	82.49	0.596	−0.06	0.32
Fe	4.29	0.15	−0.06	0.20	79.39	1.683	−0.05	0.05
Co	4.39	0.05	−0.01	0.00	75.23	1.914	−0.01	0.00
Ni	4.44	0.00	0.00	0.00	73.83	1.86	0.00	0.00
Cu	3.50	0.94	0.14	0.00	79.86	1.37	−0.05	0.31
Zn	1.35	3.09	−0.63	0.00	103.02	0.598	−0.02	0.80
Rb	0.85	3.59	2.59	0.01	587.83	0.031	0.54	2.60
Sr	1.72	2.72	−0.06	0.00	379.12	0.116	1.10	1.99
Y	4.39	0.05	−1.62	0.00	223.45	0.366	1.17	0.65
Zr	6.32	−1.88	−1.37	0.00	157.30	0.833	0.78	−0.30
Nb	7.47	−3.03	−1.36	0.36	121.37	1.702	0.29	−1.05
Mo	6.81	−2.37	−0.32	0.40	105.11	2.725	0.06	−0.70
Tc	6.85	−2.41	0.03	0.00	95.85	2.97	−0.04	−0.83
Ru	6.62	−2.18	0.02	0.00	91.68	3.208	−0.06	−0.78
Rh	5.75	−1.31	−0.04	0.00	92.95	2.704	−0.05	−0.50
Pd	3.94	0.50	0.00	0.00	99.24	1.808	−0.02	0.15
Ag	2.96	1.48	0.68	0.00	115.35	1.007	0.12	0.84
Cd	1.16	3.28	−0.24	0.00	145.43	0.467	0.33	1.34
Cs	0.83	3.61	2.84	0.01	745.67	0.020	0.46	2.61
Ba	1.86	2.58	0.01	0.00	421.77	0.103	1.16	2.02
La	4.49	−0.05	−1.46	0.00	249.93	0.243	1.03	0.53
Hf	6.35	−1.91	−2.04	0.00	149.29	1.09	0.76	−0.56
Ta	8.09	−3.65	−1.33	0.19	148.31	2.00	1.07	−0.53
W	8.66	−4.22	−0.14	0.52	107.11	3.232	0.10	−1.18
Re	8.10	−3.66	0.10	0.00	99.24	3.72	0.00	−1.19
Os	8.10	−3.66	0.06	0.00	94.51	4.18	−0.04	−1.24
Ir	6.93	−2.49	−0.07	0.00	95.58	3.55	−0.04	−0.89
Pt	5.85	−1.41	−0.22	0.00	101.93	2.783	0.02	−0.52
Au	3.78	0.66	0.33	0.00	114.37	1.732	0.17	0.50
Hg	0.69	3.75	0.04	0.00	158.41	0.382	0.41	1.67
Tl	1.87	2.57	0.14	0.00	192.80	0.359	0.77	1.67
Pb	2.04	2.40	0.08	0.00	204.49	0.430	1.08	1.91

$M(1)-M(n)$ $(n=2,3,4)$ differ from the bulk values. Taking the contributions from the volume effect [Eq. (6)] and the bonding character [Eq. (10)] together, the embrittling effect, ΔE_B^A, of an alloying addition A is now

$$\Delta E_B^A=\frac{1}{3}(E_{Coh}^A-E_{Coh}^M)+\Delta E_V^A. \tag{12}$$

Although the relation in Eq. (8) is drawn from only a few cases, it can be expected to hold in general for other alloying

additions in this high-angle boundary system. The difference between 1/3, obtained from our first-principles case studies, and 0.293, given by the $\sqrt{Z}$ theory, is only 0.04. If we take this difference as the error of the relation in Eq. (8), the relative error in the factor 1/3 is only about 12%.

C. Heat of formation for solid solutions: Macroscopic atom model

Since the unit cell we employed for computation is periodic and the lattice type of the matrix is kept as its bulk crystal, the systems under our investigation, strictly speaking, are solid solutions. The heat of formation for solid solutions can be viewed as a chemical shift of the bonding capability of the solute atoms. One difference between solid solutions and alloys is that in the former system, atoms with different sizes have to occupy equivalent lattice positions. This gives rise to an additional positive contribution, in the form of elastic energy, to the alloying enthalpy, due to the lattice deformation (or ''atomic size mismatch''). This elastic energy is discussed in Sec. II A. Since our interest is not limited to a few specific additions (in Fe or Ni), we need comprehensive thermodynamic data for the heat of formation of all the A elements in M (M=Fe and Ni) alloys. The existing experimental data is far from complete and the first-principles determination of these quantities is beyond the computational effort we can afford in the present paper. As an alternative, we employ the *macroscopic atom* model[23] to estimate the heat of an alloy with a specific concentration that is determined by our slab model.

In the *macroscopic atom* picture, the heat of formation of an alloy A in M with a concentration c_A is

$$\Delta E^A_{Sol}=(1-C_A)[1+8C_A^2\times(1-C_A)^2]\times\Delta E^A_{Sol}(0), \tag{13}$$

where C_A is

$$C_A=\frac{c_A(V^A)^{2/3}}{c_A(V^A)^{2/3}+(1-c_A)\times(V^M)^{2/3}}, \tag{14}$$

and $\Delta E^A_{Sol}(0)$ is the heat of an alloy of A in M in infinite dilution.[23] In our first-principles calculation, c_A is 1/23 for A in Fe, and 1/21 for A in Ni.

Another difference between solid solutions and alloys is that in the former case there is a structure-dependent enthalpy related the preference for metallic elements to crystalize in one of the main crystallographic structures, namely, bcc, fcc, and hcp, depending on the number of their valence electrons.[23] We use ΔE^A_{Stru} to denote the total energy difference of elemental crystal A between its ground-state structure and that of the host. Skriver[30] studied systematically the crystal structure of all the transition metals by the first-principles linear muffin-tin orbital method in the local-density approximation, and showed that with the experimental atomic volume, the energy difference between bcc and fcc is one order of magnitude larger than that between fcc and hcp. To our knowledge, there are no systematic first-principles investigations with GGA, so far. To make all (or, as many as possible,) contributions in our model to be

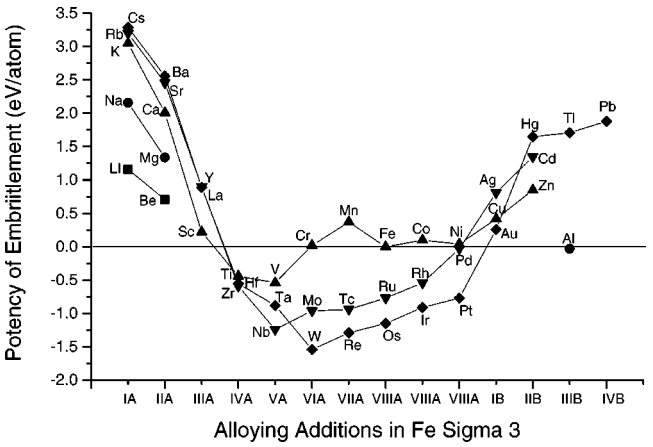

FIG. 3. Embrittlement potency of substitutional additions on the Fe $\Sigma 3(111)$ GB.

founded on the same basis, we prefer not to cite the above LDA results but to carry out full GGA calculations for all the elements under consideration. In doing so, we approximate the hcp by the fcc structure in order to save computational effort. This approximation will introduce an error to ΔE^A_{Stru}, which is about 10%.

Taking the above two corrections into account, Eq. (12) becomes

$$\Delta E^A_B=\frac{1}{3}(E^A_{Coh}-E^M_{Coh}+\Delta E^A_{Sol}+\Delta E^A_{Stru})+\Delta E^A_V. \tag{15}$$

For Mo and Pd in the Fe $\Sigma 3$ (111) GB, the model calculated values for ΔE^A_B are -0.96 and -0.03 eV, respectively. As mentioned above, our first-principles results are -0.90 and $+0.08$ eV, respectively. Note that for Mo and Pd in the Fe GB, the embrittlement potency given by Seah's pair-bonding model[6] is -1.5 and $+0.9$ eV, respectively, which are significantly greater than our results.

The model predicted embrittlement potencies of all the simple and transition metal elements as substitutional alloying additions to the Fe $\Sigma 3$ (111) and Ni $\Sigma 5$ (210) GB are listed in column 9, in Tables I and II. To be more illustrative and more readily compared, these values are plotted in Fig. 3 (for Fe) and Fig. 4 (for Ni), respectively.

III. CONFIRMATION OF THE MODEL

In order to verify our theory, we carried out first-principles calculations on the effects of $3d$ transition metal (Co), $4d$ transition metal (Ru), and $5d$ transition metals (W and Re) segregation on the cohesion of the Fe $\Sigma 3$ (111) GB and a simple metal (Ca) on the Ni $\Sigma 5$ (210) GB by using the same FLAPW method. As sketched in Fig. 1 for the Fe $\Sigma 3$ (111) GB case and Fig. 2 for the Ni $\Sigma 5$ (210) GB case, both the FS and GB were simulated by a slab model.[21] To obtain reliable values, the FS and GB systems were treated on an equal footing with high accuracy and the atomic structures of the FS and GB were also optimized in the normal direction for the cases with and without segregated atoms. Bearing this in mind, we used the same set of numerical

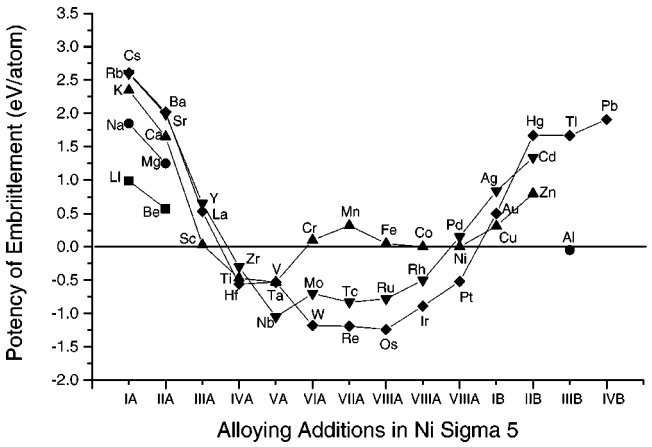

FIG. 4. Embrittlement potency of substitutional additions on the Ni $\Sigma 5$ (210) GB.

parameters (k points, plane-wave cutoff, muffin-tin radius, etc.) in the FLAPW calculations for both the FS and GB.

In the FLAPW method,[19] no shape approximations are made to the charge densities, potentials, and matrix elements. For both host and alloying additions, the core states are treated fully relativistically and the valence states are treated semirelativistically (i.e., without spin-orbit coupling). The GGA formulas for the exchange-correlation potential are from Perdew *et al.*[20]

For Co, Ru, W, and Re on the Fe $\Sigma 3$ GB, our first-principles results are $+0.05$, -0.65, -1.31, and -1.31 eV, respectively. The values calculated with the model are $+0.10$, -0.77, -1.54, and -1.29 eV, respectively. The largest discrepancy between the first-principles and the model results is about 0.2 eV in the case of W, whereas for Ca in the Ni $\Sigma 5$ (210) GB, our model gives $+1.65$ eV and the first-principles results show an embrittlement potency of $+1.4(\pm 0.2)$ eV. In general, the agreement between our phenomenological model and first-principles is quite good.

IV. SUMMARY

Starting from first principles, we formulated and developed an electronic level phenomenological theory to quantitatively predict the mechanical behavior of a substitutional metallic element in the grain boundary without carrying out full first-principles calculations, once the atomic structure of the clean grain boundary is determined. From our results, it is concluded that the strongest cohesion enhancer in the Fe $\Sigma 3$ (111) GB is W, followed by Re, Nb, and Os. The strongest cohesion enhancer in the Ni $\Sigma 5$ (210) GB is Os, followed by Re, W, and Nb. This model was tested and verified by detailed rigorous first-principles calculations on Fe and Ni based alloys. Although we have focused on two specific GB types, i.e., bcc Fe $\Sigma 3$ (111) and fcc Ni $\Sigma 5$ (210), we expect our theory to be applicable to other high boundaries in general and instructive in the quantum design of ultrahigh-strength alloys through selection of alloying elements for GB cohesion enhancement. Further calculations and modelings of the segregation energy from crystalline solution to GB are underway to next control the segregation of desired components to the boundary.

ACKNOWLEDGMENTS

Work supported by the Office of Naval Research (Grant No. N00014-94-1-0188) and a grant of Cray-T90 computer time at the NSF-supported San Diego Supercomputing Center and Cray-J90 computer time at the Arctic Region Supercomputing Center, supported by the DOD.

[1] See, e.g., C.L. Briant and S.K. Banerji, in *Embrittlement of Engineering Alloys*, edited by C.L. Briant and S.K. Banerji (Academic Press, New York, 1983), p. 21.
[2] See, e.g., A.R. Troiano, Trans. Am. Soc. Met. **52**, 54 (1960).
[3] R.H. Doremus, J. Appl. Phys. **47**, 1833 (1976).
[4] J.P. Stark and H.L. Marcus, Metall. Mater. Trans. A **8A**, 1423 (1977).
[5] D.Y. Lee, E.V. Barrera, J.P. Stark, and H.L. Marcus, Metall. Mater. Trans. A **15A**, 1415 (1984).
[6] M.P. Seah, Acta Metall. **28**, 955 (1979).
[7] P. Wynblatt and R.C. Ku, Surf. Sci. **65**, 511 (1977).
[8] J.R. Rice and J.S. Wang, Mater. Sci. Eng., A **107**, 23 (1989).
[9] M.S. Daw and M.I. Baskes, Phys. Rev. Lett. **50**, 1285 (1983).
[10] T. McMullan, M.J. Scott, and E. Zaremba, Phys. Rev. B **35**, 1076 (1987).
[11] G.S. Painter and F.W. Averill, Phys. Rev. Lett. **58**, 234 (1987).
[12] M.E. Eberhart and D.D. Vvedensky, Phys. Rev. Lett. **58**, 61 (1987).
[13] R. Wu, A.J. Freeman, and G.B. Olson, Science **265**, 376 (1994).
[14] L.P. Sagert, G.B. Olson, and D.E. Ellis, Philos. Mag. B **77**, 871 (1997); L.P. Sagert, Ph.D. thesis, Northwestern University, 1995.
[15] L.P. Zhong, R. Wu, A.J. Freeman, and G.B. Olson, Phys. Rev. B **55**, 11 133 (1997).
[16] W.T. Geng, A.J. Freeman, R. Wu, C.B. Geller, and J.E. Raynolds, Phys. Rev. B **60**, 7149 (1999).
[17] W.T. Geng, A.J. Freeman, R. Wu, and G.B. Olson, Phys. Rev. B **62**, 6208 (2000).
[18] G.B. Olson, Science **277**, 1237 (1997).
[19] E. Wimmer, H. Krakauer, M. Weinert, and A.J. Freeman, Phys. Rev. B **24**, 864 (1981), and references therein; M. Weinert, E. Wimmer, and A.J. Freeman, *ibid.* **26**, 4571 (1982).
[20] J.P. Perdew, K. Burke, and M. Ernzerhof, Phys. Rev. Lett. **77**, 3865 (1996).
[21] R. Wu, A.J. Freeman, and G.B. Olson, J. Mater. Res. **7**, 2403 (1992); G.L. Krasko and G.B. Olson, Solid State Commun. **76**, 247 (1990).
[22] H.W. King, *Alloying Behavior and Effects in Concentrated Solid Solutions* (Gordon and Breach, New York, 1966).
[23] F.R. de Boer, R. Boom, W.C.M. Mattens, A.R. Miedema, and A.K. Niessen, *Cohesion in Metals* (North-Holland, New York,

1988), p. 44.
[24] C. Kittel, *Introduction to Solid State Physics*, 4th ed. (Wiley, New York, 1971), p. 39.
[25] T. Ochs, O. Beck, C. Elsässer, and B. Meyer, Philos. Mag. A **80**, 351 (2000).
[26] T. Ochs, O. Beck, C. Elsässer, M. Mrovec, V. Vitek, J. Belak, and J.A. Moriarty, Philos. Mag. A **80**, 2405 (2000).
[27] J. Friedel, Adv. Phys. **3**, 446 (1954); D.J. Eshelby, J. Appl. Phys. **25**, 255 (1954); Solid State Phys. **3**, 19 (1956).
[28] G. Allan, in *Handbook of Surfaces and Interfaces*, edited by L. Dobrzynski (Garland SPTM, New York, 1978), and references therein.
[29] D. Spanjaard and M.C. Desjonqueres, Phys. Rev. B **30**, 4822 (1984).
[30] H.L. Skriver, Phys. Rev. B **31**, 1909 (1985).
[31] G. Bradfield, *Use in Industry of Elasticity Measurments in Metals with the Help of Mechanical Vibrations* (Her Majesty's Stationery Office, London, 1964), p. 5.